Low Resolution Mapping of the effective attenuation coefficient of the human head:
A multi-distance approach applied to high-density optical recordings

Antonio M. Chiarelli, Edward L. Maclin, Kathy A. Low, Monica Fabiani, & Gabriele Gratton

University of Illinois at Urbana-Champaign

Introduction

Near Infra-Red (NIR) light has been widely used for measuring changes in hemoglobin concentration in the human brain (functional NIR Spectroscopy, fNIRS). fNIRS is based on differential light measurements and estimation of absorption perturbation. Rather than differential measurements, another interesting application of NIR technology is tissue baseline optical properties (absorption and reduced scattering coefficients) characterization. Among other applications, baseline characterization is important to determine light propagation, which in turn affects fNIRS imaging. However, because of the highly diffusive properties of the medium, separate determination of absorption and scattering across the whole head is extremely challenging. The effective attenuation coefficient (EAC), which is related to the geometric mean of absorption and reduced scattering coefficients, can be estimated in a simpler fashion by using multi-channel light decay measurement. For depths exceeding few millimeters from the scalp, light propagation is governed by EAC, whose mapping could therefore be of great interest for the scientific community. We developed and tested an EAC topographic mapping procedure which can be applied to standard fNIRS recordings.

Methods and Results

Studies performed: Analytical simulations, Finite Element Method (FEM)[1] simulations, Real Phantom measurements, In vivo measurements on 5 participants

Analytical solution:

For a semi-infinite, homogenous medium, the continuous reflectance I(r) recorded at a distance r from a source can be approximated by the following formula [2]):

$$\ln(I(r)r^2) = k - r\mu_{eff}$$

where k is a factor that does not depend on distance and it is mainly related to source power and detector efficiency.

The equation is valid only when $r \gg \frac{1}{\mu_{eff}}$ which is around 5 mm in vivo .

EAC is defined as:

$$\mu_{eff} = \sqrt{3(\mu_a + \mu_s')} \approx \sqrt{3\mu_a\mu_s'}$$

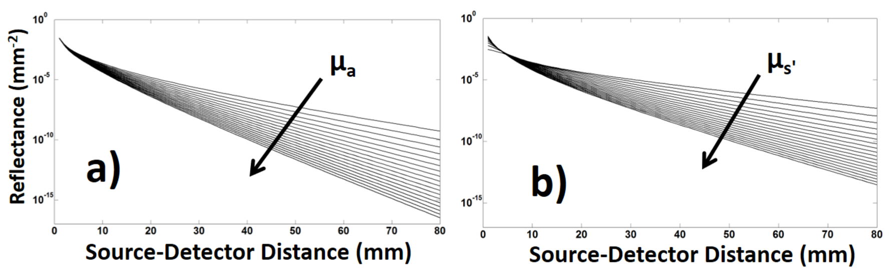

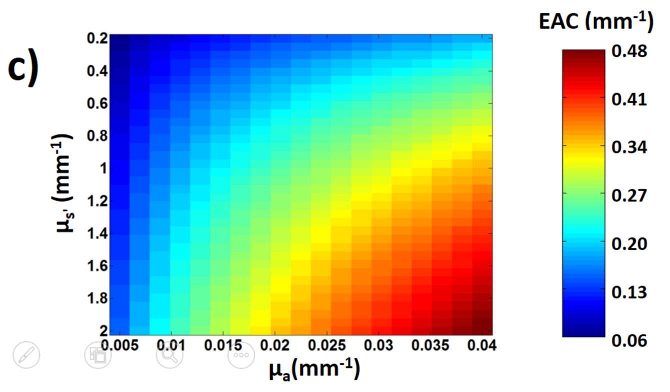

Algorithm:

1. Locate the k_{th} channel barycenter $\vec{r}_{ck}$ for the channel c_k composed by the i_{th} source s at position $\vec{r}_{si}$ and the j_{th} detector d at position $\vec{r}_{dj}$ at: $\vec{r}_{ck} = \frac{\vec{r}_{si}+\vec{r}_{dj}}{2}$ $\forall$ c $\in$ S where S is the set of all the channels considered in the measurement.
2. Estimate inter-optode distance r_k for the k_{th} channel c_k composed by the i_{th} source s at position $\vec{r}_{si}$ and the j_{th} detector d at position $\vec{r}_{dj}$ as: $r_k = \|\vec{r}_{si} - \vec{r}_{dj}\|$ $\forall$ c $\in$ S .
3. Define a neighborhood radius ρ.
4. Define a subset of Channels S_k for the k_{th} channel c_k such that the m_{th} channel $c_m \in S_k \leftrightarrow \|\vec{r}_{cm} - \vec{r}_{ck}\| < \rho$ where $S_k \subseteq S, \forall c \in S$.
5. Compute EAC_k at location $\vec{r}_{ck}$ for the channel c_k using equation 1 and the subset of channels S_k $\forall c_k$.
6. Obtain topographic images by cubic spline interpolation of the EAC_k values among all channels' barycenters $\vec{r}_{ck}$.

The number of channels considered for each EAC estimate could be adjusted by modifying the neighborhood radius ρ, thereby also affecting the resolution of the topographic image.

Procedure localization power and resolution: FEM simulations

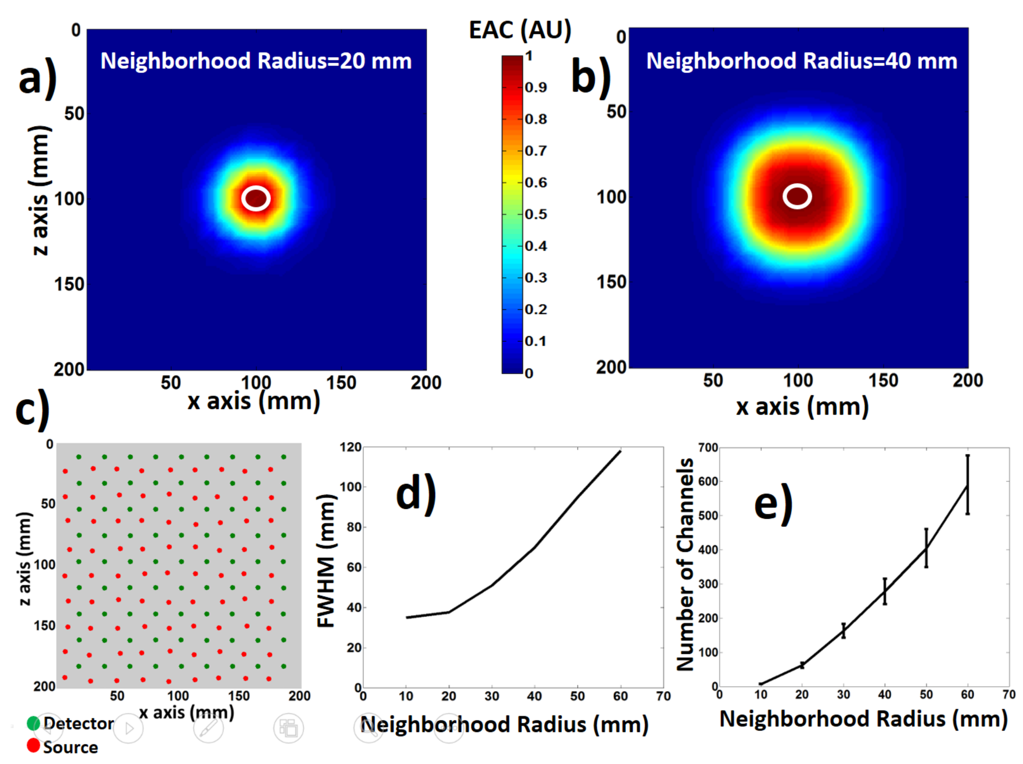

Real data limitation:

1. **Different detectors' gains; solution->** usage of shot noise estimate which is related to detected light (SNR at high frequencies, above 5 Hz).
2. **SNR plateauing; solution->**algorithm developed to find a minimum usable SNR.
3. **Optode coupling variability; solution->** Considered a source of random Gaussian noise; noise reduction through statistical procedures. (averaging, which provides a trade-off between resolution and noise reduction, and covariance analysis)

FEM simulations

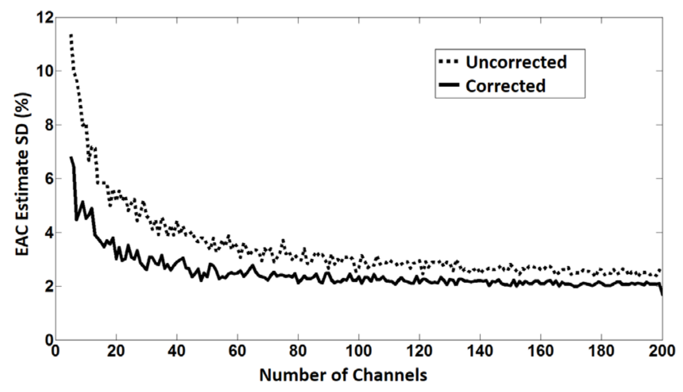

Real whole-head data (1536 channel)

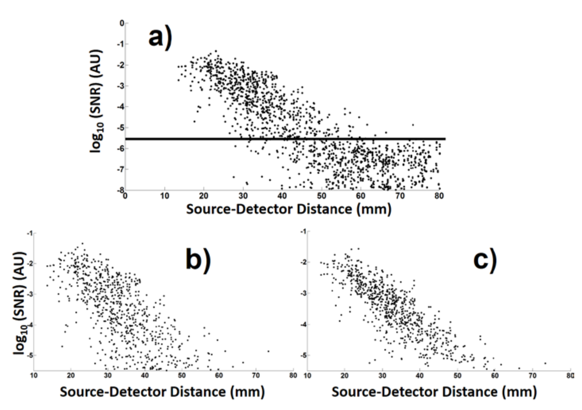

Simulated FEM vs Real data: EAC mapping

Reconstruction of a EAC inhomogeneity performed using simulated FEM data (top image) and real data (bottom image). The procedure was able to accurately quantify and localize the inhomogeneity in the EAC (white rectangle) on both simulated and real data.

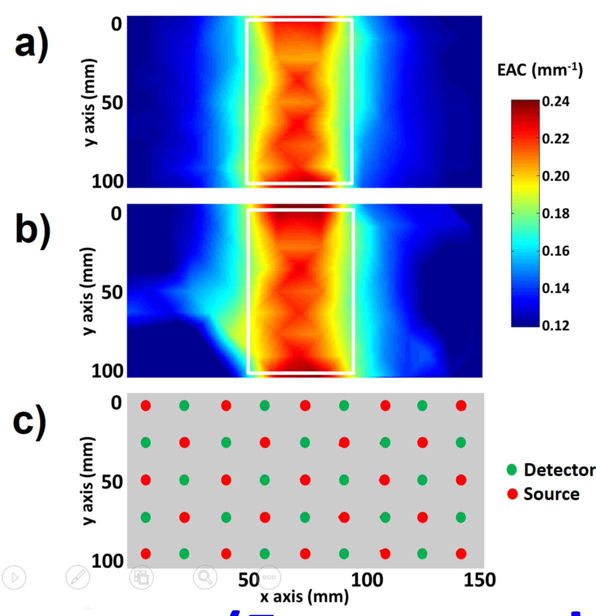

Application to in-vivo measurements (5 young subjects, ISS system, 830 nm wavelength, 1536 channel)

EAC maps showed inter-subject reliability (average r=0.85).

Moreover each subject image was correlated to the average of the other 4 (c). Higher EAC was generally measured on occipital and dorsal areas.

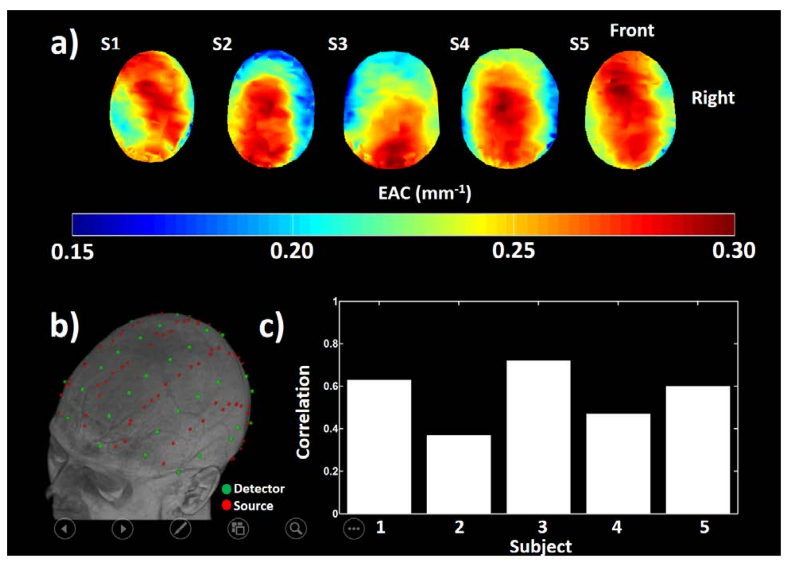

We investigated the possibility that major veins accounted for gross EAC variation across space. Baseline optical properties of T1 segmentation were taken form [3] and FEM simulations were compared to Real Results (through EAC computation). Segmented veins were added to the T1 model (veins optical properties taken from [4]), and the results obtained with new model were compared to real results. Higher correlation was found when veins were accounted for.

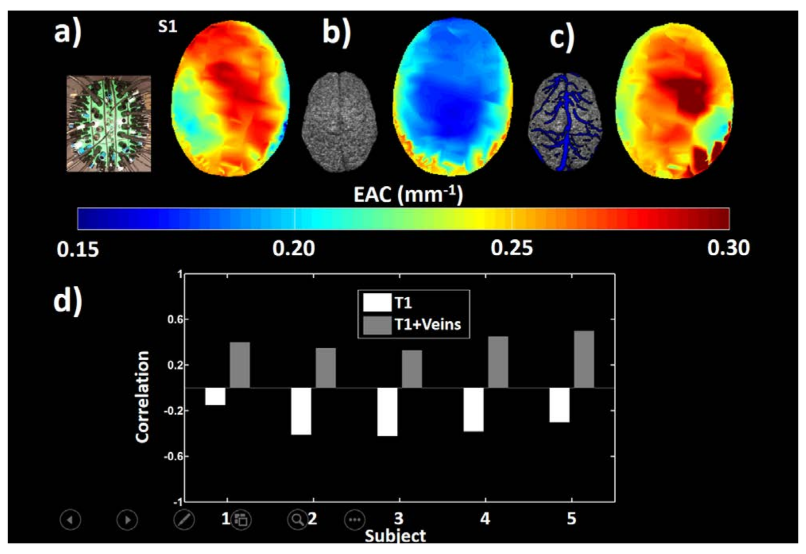

Conclusions

We developed a procedure for topographically mapping EAC in humans using an extended, high-density optical recording array. The procedure relies on the estimation of the light decay as a function of source-detector distance. This procedure does not require independent calibration data and it can be applied to continuous-wave optical recordings. This means that EAC maps with a resolution of 2-3 cm can be obtained using the same technology commonly employed for high-density fNIRS studies. Moreover, application of the procedure to human recordings indicates the importance of venous sinuses in determining regional EAC variations, a factor typically overlooked in the current literature. Empirical measurement of EAC in humans can be useful for increasing the accuracy of fNIRS data.

This work was supported by grants NIMH 5R56MH097973 (Drs. Gratton and Fabiani, PIs) and NCRR grant S10-RR029294 (Dr G. Gratton PI).

[1] H. Dehghani et al. **25**(6), 711-732 (2009); [2] D.M. Hueber et al. "In BiOS'99 Int. Biom. Opt. Symp. (pp. 618-631, 1999); [3] A. T. Eggebrecht et al. Nature photonics, **8**(6), 448-454 (2014); [4] 37S. L. Jacques. Physics in medicine and biology, **58**(11), R37 (2013).